Performance Analysis of Fission and Surface Source Iteration Method for Domain Decomposed Monte Carlo Whole-Core Calculation

YuGwon Jo and Nam Zin Cho*
Korea Advanced Institute of Science and Technology (KAIST)
291 Daehak-ro, Yuseong-gu, Daejeon, Korea 34141
**nzcho@kaist.ac.kr*

1. Introduction

For the high-fidelity whole-core reactor analysis using the continuous-energy Monte Carlo (MC) calculation, terabyte-level memory is required [1]. To overcome this excessive memory demand, the fission and surface source (FSS) iteration method was proposed [2] as a domain decomposition method (The word "iteration" is used rather than "cycle"). It is based on banking both the fission and surface sources for the next iteration. The fission sources are provided as usual, while the surface sources are provided by banking MC particles crossing local domain boundaries. The surface sources serve as boundary conditions for nonoverlapping local problems, so that each local problem can be solved independently.

In this paper, two issues in the FSS iteration are investigated. One is quantifying the waiting time of processors to receive surface source data. By using non-blocking communication, "time penalty" to wait for the arrival of the surface source data is reduced. The other important issue is underestimation of the sample variance of the tally because of additional inter-iteration correlations in surface sources. To estimate the real variances of tallies in the FSS iteration method, the history-based batch (HB) method [3] is applied. From the numerical results on a 3-D whole-core test problem, it is observed that the time penalty is negligible in the FSS iteration method and that the real variances of both pin powers and assembly powers are estimated by the HB method.

2. Methodology

2.1 Fission and Surface Source (FSS) Iteration Method using Non-Blocking Communication

For the whole-core MC calculation, the global domain is decomposed into I local domains, where the local problem for the domain D_i (i=1 to I) is given by fixed-k (also known as fixed-source) problem with incoming angular flux boundary condition. In MC calculation, incoming angular flux boundary condition can be treated as surface sources, similarly to fission sources. Local problems are iteratively solved by updating both fission source and surface sources. The fission sources are provided as usual, while the surface sources are provided by banking MC particles crossing local domain boundaries.

For domain-based parallelization, each local problem is assigned to a group of processors and solved independently. At the end of each FSS iteration, local tallies in domain D_i are gathered by a local tally server using the blocking communication, while the surface source data are sent to processors in neighboring local problems by using the non-blocking communication with the message-passage interface (MPI) parallelism [4].

2.2 Application of History-Based Batch (HB) Method to FSS Iteration Method

In this section, the HB method is applied to the FSS iteration method to estimate the real variance of the sample mean $\bar{Q}$. At the beginning of the first active iteration, both fission and surface sources are grouped into M_{HB} history-based batches with the same source size. As the FSS iteration proceeds, each group of ancestor fission and surface sources generates descendant fission and surface sources for the next iteration and form a history-based batch.

Because of normalization of the sources imposed on each iteration, the initial source weight W^l for both fission and surface sources is determined as:

$$W^l = \frac{N}{N_f^l}\ , \text{ with } N_f^l = \sum_{i=1}^{I}\left(N_{i,f}^l\right), \tag{1}$$

where l is the FSS iteration index, N is the nominal fission source size of each iteration, $N_{i,f}^l$ is the number of fission sources in local domain i at iteration l.

The history-based batch tallies Q^m for the history-based batch index m (m=1 to M_{HB}) are estimated as:

$$Q^m = \frac{1}{L_{active}(N/M_{HB})}\sum_{l=1}^{L_{active}}\sum_{n\in m} f_l^m Q_{l,n}\ , \tag{2}$$

where L_{active} is the number of active iterations, $Q_{l,n}$ is a tally from the source (or history) index n at iteration l, and f_l^m is the weight correction factor to preserve the sample mean $\bar{Q}$ defined as:

$$f_l^m = \frac{N_f^l / M_{HB}}{N_f^{l,m}}\ . \tag{3}$$

In Eq. (3), $N_f^{l,m}$ is the number of fission sources included in the m-th history-based batch at iteration l.

Then, the sample variance of the sample mean for the history-based batch tallies is obtained as:

$$\sigma^2[\bar{Q}_{HB}] = \frac{1}{M_{HB}(M_{HB}-1)}\sum_{m=1}^{M_{HB}}(Q^m - \bar{Q}_{HB})^2\ , \tag{4}$$

where $\bar{Q}_{HB}$ is the sample mean of history-based batch tallies obtained as:

$$\bar{Q}_{HB} = \frac{1}{M_{HB}} \sum_{m=1}^{M_{HB}} Q^m = \frac{1}{L_{active} N} \sum_{l=1}^{L_{active}} \sum_{m=1}^{M_{HB}} \sum_{n \in m} f_l^m Q_{l,n} \,. \qquad (5)$$

Since Eq. (4) is free from the variance bias, the real variance of the sample mean can be estimated by Eq. (4) by assuming $\bar{Q}_{HB} = \bar{Q}$.

3. Numerical Results

The test problem is a 3-D continuous-energy whole-core problem modified from the Benchmark for Evaluation and Validation of Reactor Simulations (BEAVRS) [5]. Figs. 1 and 2 show the radial configurations, while Fig. 3 shows the axial configuration of the test problem. The material compositions and densities used are the same with those of Ref. [5]. NJOY version 99.364 [6] is used to generate continuous-energy cross section library at 600K using ENDF/B-VII.0. The continuous-energy MC calculations are performed by the in-house research code McBOX [7].

Fig. 4 shows three different test cases for domain decomposition, where Case 1 is the conventional power iteration without domain decomposition, Case 2 is the FSS iteration with 4 local domains showing natural load-balance property, and Case 3 is the FSS iteration with 16 local domains showing load-imbalance property.

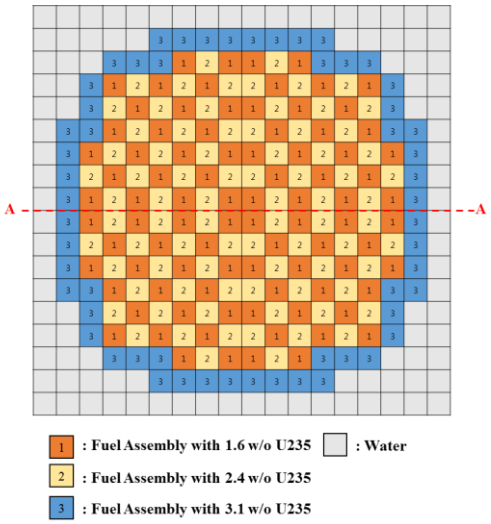

Fig. 1. Radial configurations of whole-core showing enrichment loading pattern.

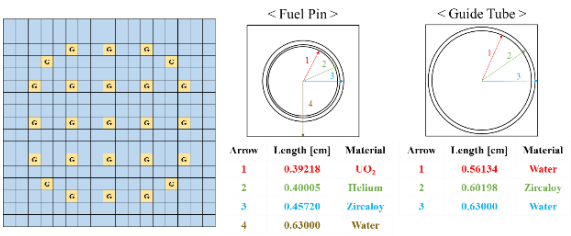

Fig. 2. Radial configurations of fuel assembly showing locations of guide tubes.

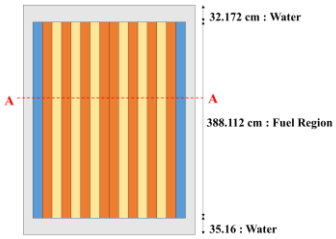

Fig. 3. Axial configurations of whole-core (A-A cross section in Fig. 1).

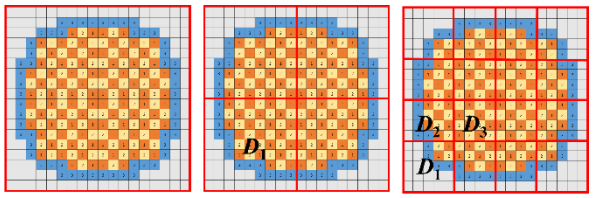

Fig. 4. Three test cases for domain decomposition using the FSS iteration method.

Total 80 processors are assigned as in Table I, where the computing nodes are interconnected by Intel® 82576 Gigabit Ethernet Controller, and OpenMPI version 1.8.1 is used for MPI parallelism.

Table I: Processor assignment for three test cases

	Case 1	Case 2	Case 3
No. of domains	1	4	16
No. of processors* per domain	80	20	5

* Intel® CoreTM i7-5820K @ 3.30 GHz

For all test cases, MC calculations are performed with 60 inactive iterations, 400 active iterations, and 1,000,000 fission sources per iteration. During inactive iterations, the partial current-based coarse-mesh finite difference (p-CMFD) acceleration method [8] is applied to all cases. It should be noted that the p-CMFD acceleration causes large fluctuations in source distributions. To stabilize the source distributions, the "adaptive p-CMFD acceleration" is applied; an arbitrary factor α for the "generalized p-CMFD method" [9] varies linearly from 0 to -60 during inactive iterations, so that the fluctuations in the source distributions become smaller as the iteration proceeds at the expense of the acceleration speed. The coarse-mesh size for the p-CMFD method is set as an assembly size with 20 divisions in the axial direction.

3.1 Source Convergence Check

To check fission and surface source convergence of the FSS iteration method, both the Shannon entropy of fission source distribution and the ratio of the total number of surface sources to the total number of fission sources are monitored. Fig. 5 shows the Shannon entropies of the three test cases, where the bins for Shannon entropy are set as an assembly size with 18 divisions in the axial direction. The reference Shannon entropy is obtained by the average of the Shannon entropies from iteration 401 to iteration 1400 in the conventional power iteration method.

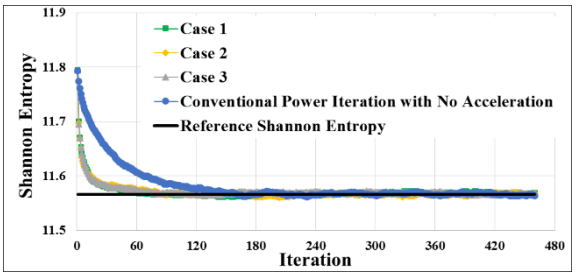

Fig. 5. Shannon entropies of fission source distributions

Fig. 6 shows the ratio of the total number of surface sources to the total number of fission sources in Cases 2 and 3. The average of the ratios over active iterations are 0.1605 and 0.4641 for Cases 2 and 3, respectively.

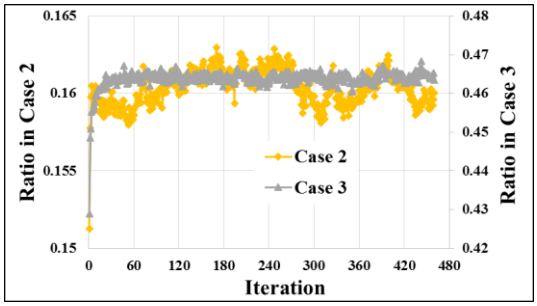

Fig. 6. Ratio of the total number of surface sources to the total number of fission sources in Cases 2 and 3.

3.2 Computing Time Analysis

In Table II, $\bar{t}_{track,i}$ and $\bar{t}_{penalty,i}$ represent the averages of the source-tracking times and the time penalties over the processors assigned to local domain i and the other local domains in symmetric locations, respectively; $\bar{N}_i$ represents the average number of sources per processor assigned to local domain i and the other local domains in symmetric locations; $\sigma_S[t_{track,i}]$, $\sigma_S[t_{penalty,i}]$, and $\sigma_S[N_i]$ represent the sample standard deviations of each quantity.

Table II. Comparison of the source-tracking times [sec], the time penalties [sec], and the number of sources of three test cases at the first active iteration

	$\bar{t}_{track,i}$ ($\sigma_S[t_{track,i}]$)	$\bar{t}_{penalty,i}$ ($\sigma_S[t_{penalty,i}]$)	$\bar{N}_i$ ($\sigma_S[N_i]$)
Case 1	1.67 (0.03)	n/a	12515 (9)
Case 2[1)]			
Local Domain D_1	1.69 (0.08)	5.74E-05 (2.08E-05)	14541 (554)
Case 3[2)]			
Local Domain D_1	0.80 (0.05)	3.37E-05 (2.33E-05)	9464 (599)
Local Domain D_2	1.84 (0.14)	6.20E-05 (3.04E-05)	19478 (1450)
Local Domain D_3	2.17 (0.12)	9.33E-05 (3.46E-05)	25103 (1263)

[1)]Local domain D_1 is denoted in Fig. 4 (Case 2).
[2)]Local domains D_1, D_2, and D_3 are denoted in Fig. 4 (Case 3).

3.3 Real Variance Analysis

To obtain the real variance, 30 independent batch runs are performed for each test case. To distinguish standard deviations obtained by different ways, the following notations are used; σ_{app} denotes the apparent standard deviation; σ_{HB} denotes the sample standard deviation obtained by Eq. (4); σ_{real} denotes the real standard deviation. Note that the number of history-based batches used to calculate σ_{HB} is 50. Figs. 7 and 8 show the standard deviations of the pin power and assembly power distributions, respectively.

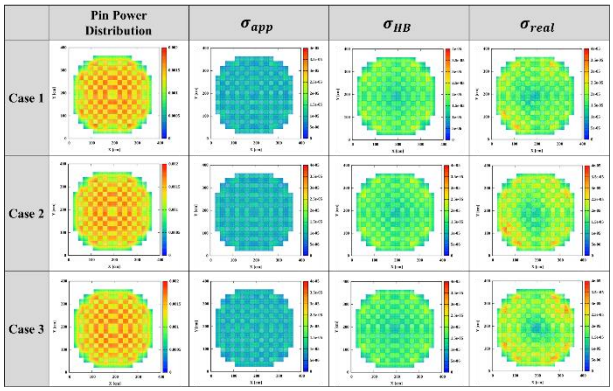

Fig. 7. Pin power distributions and their standard deviations for three test cases.

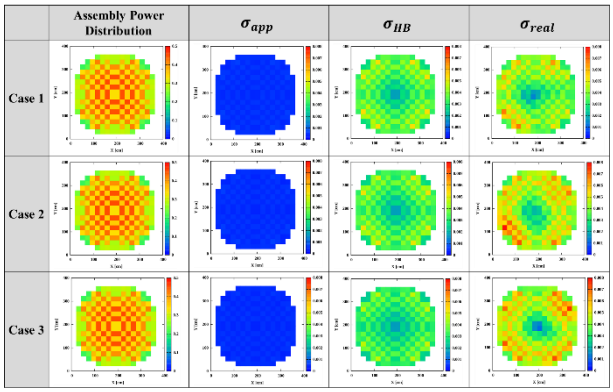

Fig. 8. Assembly power distributions and their standard deviations for three test cases.

To compare the standard deviations of the pin power and assembly power distributions easily, Table III shows the averages of the standard deviations; $\bar{\sigma}_{app}$, $\bar{\sigma}_{HB}$, $\bar{\sigma}_{real}$, and the average ratios; $\bar{r}_{app}$ and $\bar{r}_{HB}$ which represent the averages of $\sigma_{real}/\sigma_{app}$, $\sigma_{real}/\sigma_{HB}$, respectively. Compared to the $\bar{r}_{app}$ values, the $\bar{r}_{HB}$ values are much closer to unity, which means that the HB method estimates the real variances very well. It is noted that, for Case 1, the HB method estimates the real variances within 90% confidence interval. However, $\bar{r}_{HB}$ values show some deviations from unity and the deviations become larger for finer divisions of local domains. Some discussions on this observation are given in Section 4.

Table III. Comparison of the standard deviations [pcm] of pin power and assembly power distributions for three test cases

		$\bar{\sigma}_{app}$	$\bar{\sigma}_{HB}$	$\bar{\sigma}_{real}$ (90% Confidence Interval)	$\bar{r}_{app}$	$\bar{r}_{HB}$
Pin	Case 1	0.95	1.64	1.78 (1.47, 2.28)	1.88	1.08
	Case 2	0.95	1.61	1.97 (1.63, 2.52)	2.08	1.22
	Case 3	0.96	1.53	1.99 (1.64, 2.54)	2.08	1.29
Assembly	Case 1	47	349	395 (326, 506)	8.45	1.12
	Case 2	45	337	452 (373, 579)	9.94	1.34
	Case 3	43	310	455 (375, 582)	10.5	1.46

Table IV compares the standard deviations of the eigenvalues for three test cases. The average of the eigenvalues obtained by 30 independent batch runs is denoted as $\bar{k}_{eff}$, and r_{app} is the ratio of the real to apparent standard deviations. It is seen that the multiplication factor is almost free from the variance bias.

Table IV. Comparison of standard deviations [pcm] of the eigenvalues for three test cases

	$\bar{k}_{eff}$ [1)]	σ_{app}	σ_{real} (90% Confidence Interval)	r_{app}
Case 1	1.06408	4.13	4.23 (3.49, 5.41)	1.02
Case 2	1.06407	4.17	4.14 (3.42, 5.30)	0.99
Case 3	1.06406	4.60	4.60 (3.80, 5.89)	1.10

[1)]The eigenvalues are estimated by the ratio method based on the collision estimator in Ref. [2].

4. Conclusions

In this paper, two issues in the FSS iteration method, i.e., the waiting time for surface source data and the variance biases in local tallies are investigated for the domain decomposed, 3-D continuous-energy whole-core calculation. For those purposes, three cases; Case 1 (1 local domain), Case 2 (4 local domains), Case 3 (16 local domains) are tested. For both Cases 2 and 3, the time penalties for waiting are negligible compared to the source-tracking times. However, for finer divisions of local domains, the loss of parallel efficiency caused by the different number of sources for local domains in symmetric locations becomes larger due to the stochastic errors in source distributions. For all test cases, the HB method very well estimates the real variances of local tallies. However, it is also noted that the real variances of local tallies estimated by the HB method show slightly smaller than the real variances obtained from 30 independent batch runs and the deviations become larger for finer divisions of local domains. The parametric study in terms of the number sources in each history-based batch, denoted as batch size in Ref. [3] shows that the real variance estimated by the HB method can be smaller than the real variance from the independent batch runs for a small batch size in a large dominance ratio problem. The batch size used for the HB method may not be large enough to accurately estimate the real variance in this test problem.

In conclusion, the waiting time for surface source data is negligible in the FSS iteration method, and the loss of parallel efficiency caused by the different number of sources can be reduced by the source splitting scheme discussed in Ref. [2]. To estimate the real variances of local tallies, a large batch size would be required for fine divisions of the local domains.

References

[1] K. Smith and B. Forget, "Challenges in the Development of High-Fidelity LWR Core Neutronics Tools," M&C 2013, Sun Valley, Idaho, May 5-9, 2013.
[2] Y.G. Jo and N. Z. Cho, "Fission and Surface Source Iteration Method for Domain Decomposed Monte Carlo Whole-Core Calculation," *Nucl. Sci. Eng.*, **182**, 181-196 (2016).
[3] H. J. Shim S. H. Choi, and C. H. Kim, "Real Variance Estimation by Grouping Histories in Monte Carlo Eigenvalue Calculations," *Nucl. Sci. Eng.*, **176**, 58-68 (2014).
[4] E. Gabriel, et al., "Open MPI: Goals, Concept, and Design of a Next Generation MPI Implementation," Proc. 11th European Parallel Virtual Machine/Message Passing Interface Users' Group Mtg., Budapest, Hungary, September 19-21, 2004.
[5] N. Horelik, et al., "Benchmark for evaluation and validation of reactor simulation (BEAVRS)," Proc. M&C 2013, Sun Valley, USA, May 5-9, 2013.
[6] R. E. MacFarlane, S. Kahler, "Methods for Processing ENDF/B-VII with NJOY," *Nuclear Data Sheets*, **111**, 2739 (2010).
[7] Y.G. Jo and N. Z. Cho, "McBOX - A Continuous-Energy Monte Carlo Code for Neutronics Analysis in 3-D Geometry," Korea Advanced Institute of Science and Technology (KAIST), in progress.
[8] S. Yun and N.Z. Cho, "Acceleration of Source Convergence in Monte Carlo k-Eigenvalue Problem via Anchoring with a p-CMFD Deterministic Method," *Ann. Nucl. Energy*, **37**, 1649-1658 (2010).
[9] Y.G. Jo and N.Z. Cho, "Investigation of Some Variations of p-CMFD Acceleration Method in Continuous-Energy Monte Carlo Calculation," Trans. Kor. Nucl. Soc. Autumn Mtg, Pyeongchang, Korea, October 30-31, 2014.